



Statistical characters of synchronization-optimized oscillator networks

Tatsuo Yanagita[†] and Alexander S. Mikhailov[‡]

[†]Research Institute for Electronic Science, Hokkaido University,
 Sapporo 001-0020, Japan

[‡]Fritz-Haber-Institut der Max-Planck-Gesellschaft
 Faradayweg 4-6, 14195 Berlin, Germany
 Email: yanagita@nsc.es.hokudai.ac.jp

Abstract—Starting with an initial random network of oscillators with a heterogeneous frequency distribution, its autonomous synchronization ability can be largely improved by appropriately rewiring the links between the elements. Ensembles of synchronization-optimized networks with different connectivities are generated and their statistical properties are studied.

1. Introduction

In the last decade, much interest has been attracted to studies of complex networks consisting of dynamical elements involved in a set of interactions [1]. Particular attention has been paid to problems of synchronization in network-organized oscillator systems [2, 3]. Investigations focused on understanding the relationship between the topological structure of a network and its collective synchronous behavior [4]. Recently, it has also been shown that the ability of a network to give rise to synchronous behavior can be greatly enhanced by exploiting the topological structure emerging from the growth processes [5]. However, full understanding of how the network topology affects synchronization of specific dynamical units is still an open problem.

One possible approach is to use evolutionary learning mechanisms in order to construct networks with prescribed dynamical properties. Several models have been explored, where dynamical parameters were modified in response to the selection pressure via learning algorithms, in such a way that the system evolved toward a specified goal [6, 7]. In our study, this approach is employed to design phase oscillator networks with synchronization properties. We consider adaptive evolution of a network of coupled heterogeneous phase oscillators. The question is how to connect a set of phase oscillators with given natural frequencies, so that the resulting network would exhibit the strongest synchronization, under the constraint that the total number of available links is fixed.

To design optimal networks, stochastic Markov Chain Monte Carlo (MCMC) method with replica exchange is used by us. Large ensembles of optimal networks are constructed and their common statistical properties are analyzed.

2. Model and the Optimization Method

We consider N oscillators with different natural frequencies placed onto the nodes of a network. The evolution of this system is given by

$$\frac{d\theta_i}{dt} = \omega_i + \frac{\lambda}{N} \sum_{j=1}^N w_{i,j} \sin(\theta_j - \theta_i), \quad (1)$$

where ω_i is the natural frequency of oscillator i and λ is the coupling strength. The weights $w_{i,j}$ define the adjacency matrix \mathbf{w} of the interaction network: $w_{i,j} = 1$ if oscillator i interacts with oscillator j , and $w_{i,j} = 0$ otherwise. The adjacency matrix is generally asymmetric.

To quantify synchronization of the oscillators, the Kuramoto order parameter

$$r(t) = \frac{1}{N} \left| \sum_{i=1}^N \exp(i\theta_i) \right| \quad (2)$$

is employed. Under perfect synchronization, we have $r = 1$, whereas $r \sim O(N^{-1/2})$ in absence of coupling for randomly drawn natural frequencies. A second-order transition takes place at some critical coupling strength λ_c from the desynchronized to the synchronized states [8].

To measure the degree of synchronization, we numerically integrate Eq. (1) for given initial conditions $\theta_i(t = 0) \in [0, 2\pi)$ and calculate the average modulus of $r(t)$ over a long time T ,

$$R(\mathbf{w}) = \left\langle \frac{1}{T} \int_0^T r(t) dt \right\rangle_{init}, \quad (3)$$

where $\langle \dots \rangle_{init}$ represents an average over many realizations with different initial conditions $\theta_i(0)$.

Our aim is to determine the network \mathbf{w} which would exhibit the highest degree of synchronization, provided that the total number of links is fixed and a set of natural frequencies is given. The network construction can be seen as an optimization problem. The optimization task is to maximize the order parameter and, possibly, bring it to unity by changing the network \mathbf{w} . An approximate standard approach to the problems of complex combinatorial optimization, such as the traveling salesman problem, is provided by

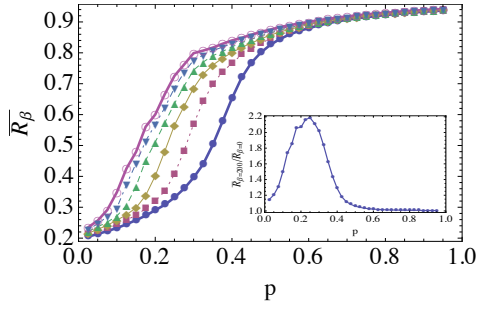


Figure 1: Average order parameters as functions of the network connectivity p . The filled circles are for the replica β_0 , i.e., the ensemble of randomly rewired networks. The squares, diamonds, triangles, inverted triangles, and open circles are for replicas with $\beta = 40, 80, 120, 160$, and 200 , respectively. Inset: Ratio of the average order parameters for the synchronization-optimized ensemble with the inverse temperature β_M and for $\beta_0 = 0$. The parameters are $p = 0.2, N = 20, \lambda = 1.0, \gamma = 0.3, M = 21, \delta\beta = 10$.

the method of simulated annealing. However, we are interested in the *statistical properties* of the synchronization-optimized networks rather than in a search for the best-optimized network. If multiple samples are generated using conventional optimization methods such as simulated annealing, it is difficult to control the probability of the repeated appearance of the same (or similar) items in the obtained set of samples.

To study statistical ensembles of optimized networks, the MCMC method [9] which has previously been applied to dynamical systems, [10, 11, 12], will be used. The canonical ensemble average of a network function $f(\cdot)$ is introduced as

$$\overline{f}_\beta = \sum_{\mathbf{w}} \frac{f(\mathbf{w}) \exp[\beta R(\mathbf{w})]}{Z(\beta)}, \quad (4)$$

where $Z(\beta) = \sum_{\mathbf{w}} \exp(\beta R(\mathbf{w}))$ is the partition function and the parameter β plays the role of the inverse temperature.

Hence, the problem is reduced to sampling from the ensemble with the Gibbs distribution $\exp(\beta R(\mathbf{w}))$. Such ensemble can be generated, for example, by using the Metropolis algorithm [13], which is the simplest implementation of the MCMC method. This Metropolis algorithm appears to provide a simple and universal way of generating the Gibbs network distribution. However, the efficiency of such algorithm gets worse when β increases, particularly in the case of a highly jagged landscape $R(\mathbf{w})$. This deficiency can be eliminated by using instead the replica exchange Monte Carlo (REMC) algorithm [14].

In a REMC simulation, a number of replicas $\{\mathbf{w}_m\}$ with different inverse temperatures β_m are evolved in parallel. At regular evolution time intervals, the performances of a randomly selected, adjacent pair of replicas are compared. The running configurations of the two selected replicas are

exchanged with the probability $\min[1, \exp(\Delta\beta\Delta R)]$, where $\Delta\beta = \beta_{m+1} - \beta_m$ is the difference of the inverse temperatures of the pair and $\Delta R = R(\mathbf{w}_{m+1}) - R(\mathbf{w}_m)$ is the difference of their performances.

Explicitly, the algorithm is defined as follows:

1. The states of replicas $\{\mathbf{w}_m^0\}$ are initialized by random networks (which is chosen as a random Erdős-Rényi network).
2. The candidate for the next network \mathbf{w}'_m at iteration step n is obtained from the current network $\mathbf{w}_m^{(n)}$ by rewiring one of its links. A randomly chosen link is moved to a randomly chosen link vacancy, so that the total number of links remains conserved.
3. The evolution equations (1) for the network \mathbf{w}'_m are integrated using the standard Euler algorithm. The order parameter is then calculated and averaged over the time interval $t \in [0, T]$ and over a fixed number of realizations starting from different random initial conditions. Thus, the synchronization property $R(\mathbf{w}'_m)$ of the candidate network is determined.

4. Next, a random number $x \in [0, 1]$ is uniformly drawn. If

$$x < \frac{\exp(\beta R(\mathbf{w}'_m))}{\exp(\beta R(\mathbf{w}_m^{(n)}))},$$

the candidate is accepted and taken as $\mathbf{w}_m^{(n+1)} = \mathbf{w}'_m$; otherwise nothing is changed, so that $\mathbf{w}_m^{(n+1)} = \mathbf{w}_m^{(n)}$.

5. At regular evolution time intervals, the performances of a randomly selected, adjacent pair of replicas are compared. The running configurations of the two selected replicas are exchanged with the probability

$$\min\left[1, \exp\left\{(\beta_{m+1} - \beta_m)(R(\mathbf{w}_{m+1}^{(n+1)}) - R(\mathbf{w}_m^{(n+1)}))\right\}\right].$$

6. Return to step (2) until the statistical average Eq. (4) converges.

3. Numerical analysis

To determine the synchronization degree of a given network at each iteration step of the optimization procedure, Eq. (1) was numerically integrated with the time increment $\Delta t = 0.05$. Averaging over five independent realizations started from different random initial conditions has been furthermore performed at each iteration step. Oscillator ensembles of sizes $N = 10$ and 20 were considered. Natural frequencies of the oscillators were always chosen as $\omega_i = -\gamma + 2\gamma i/N$, so that they uniformly distributed within the interval $[-\gamma, \gamma]$. For time averaging, intervals of length $T = 100$ and 200 were typically used. The results did not significantly depend on T when sufficiently large lengths T were taken. Using the order parameter, graphs \mathbf{w} were sampled by the REMC optimization method. In parallel, evolution of M replicas with the inverse temperatures

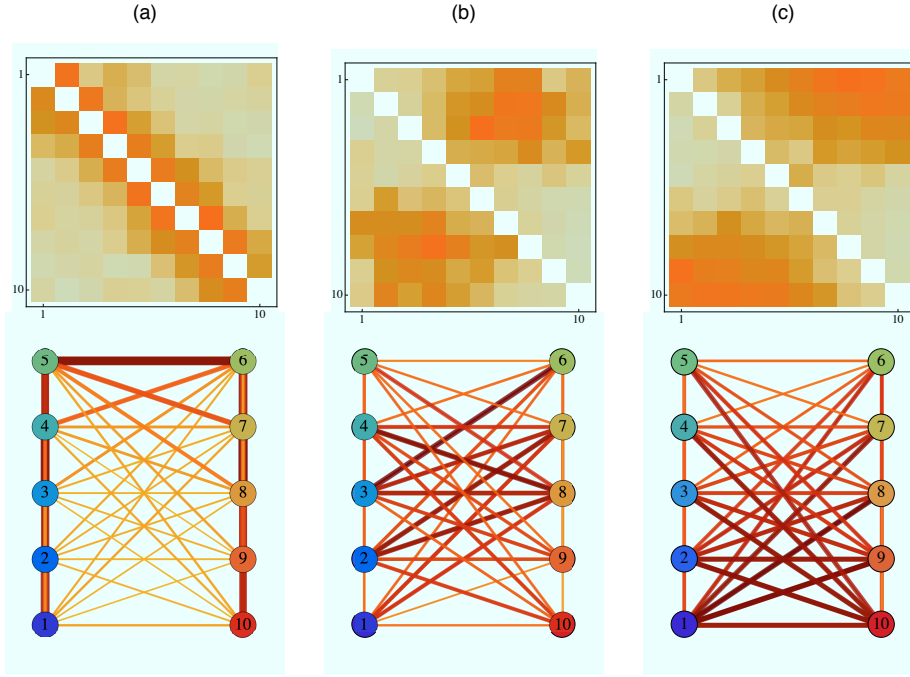


Figure 2: Upper panels show adjacent matrices averaged over the Gibbs ensemble of synchronization-optimized networks [see Eq. (5)]. The darker color of a matrix element indicates the higher probability of the respective connections between the elements. Lower panels display the corresponding network averaged over the Gibbs ensemble. Numbers in the circles show indexes of the oscillators. The thickness of the lines connecting the nodes is proportional to the frequency of links between them. The network connectivities are (a) $p = 0.05$, (b) 0.2 , and (c) 0.3 .

$\beta_m = \delta\beta \times m$, $m = 0, 1, \dots, M$ was performed (with $M = 21$ and $\delta\beta = 10$). At each five Monte Carlo steps (mcs), the performances of a randomly chosen pair of replicas were compared and exchanged, as described above. For display and statistical analysis, sampling at each every 50 mcs after a transient of 5000 mcs has been undertaken.

Hereafter, we investigate how the synchronization-optimized network change with increasing the network connectivity $p = K/N(N - 1)$, where K is off-diagonal elements of the adjacency matrix.

3.1. Optimization at different temperatures

Synchronization-optimized networks were obtained by running the evolutionary optimization. In this process, the order parameter was progressively increasing until a stationary state has been achieved. When using replicas with the larger inverse temperature β , the larger values of the order parameter could be reached, although the optimization process was then slower. After the transients, statistical averaging of the order parameter over the ensemble with the Gibbs distribution has been performed, according to Eq. (4).

In Fig. 1(a), the averaged order parameter \bar{R} is displayed as a function of the connectivity p for several different inverse temperature β . The solid circle symbols show the

averaged order parameter corresponding to the replica with $\beta_0 = 0$, i.e., for an infinitely high temperature. We see that the averaged order parameter increases with the network connectivity p even if the networks are produced by only random rewiring. The open circles show the average order parameters for the ensemble corresponding to the replicas with the lowest inverse temperature β_M . Generally, greater order parameters are obtained by running evolution at higher inverse temperatures β at any network connectivity p . At each connectivity p , the order parameter is gradually increased with increasing β and is approximately saturated at β_M . This means that, even if one further increases β , only slight improvements of the averaged order parameter can be expected. Thus, the networks sampled by the replica with the largest inverse temperature β_M are already yielding a representative optimal ensemble.

Figure 1(b) shows, depending on the network connectivity p , the ratio $\bar{R}_{\beta_M}/\bar{R}_{\beta_0}$ of the averaged order parameters sampled by the optimal network ensemble with β_M to those obtained for the ensemble with purely random rewiring. Since there is no room for the improvement of the order parameter when the number of links is small, the ratio tends to unity as the connectivity p is decreased. On the other hand, when $p = 1$, global coupling is realized, for which, under the chosen coupling strength, full synchronization occurs. As evidenced by this figure, the difference between the syn-

chronization capacities of the optimized and random networks is most pronounced at the intermediate connectivities p .

3.2. Architectures of Synchronization-Optimized Networks

When the connectivity p is small, typical structure of synchronization-optimized networks usually represent chain fragments. At a higher connectivity, the network becomes more complexly organized.

To statistically characterize the architecture of constructed networks, ensemble averages of their adjacency matrices over the Gibbs ensemble, i.e.,

$$\overline{\mathbf{w}}_{\beta} = \sum_{\mathbf{w}} \mathbf{w} \exp(\beta R(\mathbf{w})) / Z(\beta), \quad (5)$$

for different connectivities p were computed for $\beta = \beta_M$, as shown in Fig. 2. Clearly, the optimal network structure is changing with the number of links. When the number of links is small, the elements of the mean adjacency matrix, obtained by averaging over many realization from the synchronization-optimized ensemble, are large near the diagonal. Hence, elements with close natural frequency tend to connect and form a chain fragment. Moreover, oscillators with the natural frequencies near the center of the interval are often connected. Increasing the number of links, the network becomes more complicated and off-diagonal elements begin to dominate instead. The network with the larger p tends to have interlaced structures, seen in Figs. 2(b) and 5(c), where the oscillators with roughly opposite natural frequencies are coupled.

4. Summary

We have designed synchronization-optimized networks with a fixed number of links for a heterogeneous oscillator population. This has been done by using the Markov chain stochastic Monte Carlo method complemented by the replica exchange algorithm. A transition from the linear to bipartite-like networks has been found under increasing the number of links. At low connectivity, synchronization-optimized networks typically represent small chains connecting oscillators with close natural frequencies. As the number of links increases, the networks become interlaced and oscillators with opposite natural frequencies tend to be connected. Therefore, synchronization-optimized network begin to resemble bipartite graphs.

Acknowledgments

This study has been partially supported by the Ministry of Education, Science, Sports and Culture, Grant-in-Aid for Scientific Research (Grant No. 21540376) and the Volkswagen Foundation (Germany).

References

- [1] R. Albert and A.L. Barabási, “Statistical mechanics of complex networks,” *Rev. Mod. Phys.*, vol.74, no.1, pp.47–97, Jan 2002.
- [2] S. Manrubia, A. Mikhailov, and D. Zanette, *Emergence of Dynamical Order: Synchronization Phenomena in Complex Systems*, World Scientific, Singapore, 2004.
- [3] A. Arenas, A. Diaz-Guilera, J. Kurths, Y. Moreno, and C. Zhou, “Synchronization in complex networks,” *Phys. Rep.*, vol.469, pp.93–153, 2008.
- [4] S. Boccaletti, V. Latora, Y. Moreno, M. Chavez, and D.U. Hwang, “Complex networks: Structure and dynamics,” *Phys. Rep.*, vol.424, no.4-5, pp.175 – 308, 2006.
- [5] D.U. Hwang, M. Chavez, A. Amann, and S. Boccaletti, “Synchronization in complex networks with age ordering,” *Phys. Rev. Lett.*, vol.94, no.13, p.138701, Apr 2005.
- [6] M. Ipsen and A.S. Mikhailov, “Evolutionary reconstruction of networks,” *Phys. Rev. E*, vol.66, no.4, p.046109, Oct 2002.
- [7] M. Brede, “Locals vs. global synchronization in networks of non-identical kuramoto oscillators,” *Eur. Phys. J. B*, vol.62, pp.87–94, 2008.
- [8] Y. Kuramoto, *Chemical Oscillations, Waves, and Turbulence*, Springer, 1984.
- [9] D. Landau and K. Binder, *A Guide to Monte Carlo Simulations in Statistical Physics*, Cambridge University Press, 2005.
- [10] M. Kawasaki and S.I. Sasa, “Statistics of unstable periodic orbits of a chaotic dynamical system with a large number of degrees of freedom,” *Phys. Rev. E*, vol.72, p.037202, 2005.
- [11] J. Tailleur and J. Kurchan, “Probing rare physical trajectories with Lyapunov weighted dynamics,” *Nature Physics* 3, vol.3, pp.203–207, 2007.
- [12] T. Yanagita and Y. Iba, “Exploration of order in chaos using the replica exchange monte carlo method,” *J. Stat. Mech.*, vol.2, pp.02043–02058, 2009.
- [13] N. Metropolis, A. Rosenbluth, M. Rosenbluth, A. Teller, and E. Teller, “Equations of state calculations by fast computing machines,” *J. Chem. Phys.*, vol.21, pp.1087–1091, 1953.
- [14] K. Hukushima and K. Nemoto, “Exchange Monte Carlo method and application to spin glass simulations,” *J. Phys. Soc. Jpn.*, vol.65, pp.1604–1611, 1996.